# NATIONAL ADVISORY COMMITTEE FOR AERONAUTICS

**TECHNICAL NOTE 2305**

# AN ANALYTICAL AND EXPERIMENTAL INVESTIGATION OF THE SKIN FRICTION OF THE TURBULENT BOUNDARY LAYER ON A FLAT PLATE AT SUPERSONIC SPEEDS

By Morris W. Rubesin, Randall C. Maydew,
and Steven A. Varga

Ames Aeronautical Laboratory
Moffett Field, Calif.


Washington
February 1951

NATIONAL ADVISORY COMMITTEE FOR AERONAUTICS

TECHNICAL NOTE 2305

# AN ANALYTICAL AND EXPERIMENTAL INVESTIGATION OF THE SKIN FRICTION OF THE TURBULENT BOUNDARY LAYER ON A FLAT PLATE AT SUPERSONIC SPEEDS

By Morris W. Rubesin, Randall C. Maydew, and Steven A. Varga

## SUMMARY

A review is presented of turbulent-boundary-layer analyses and experimental data for average skin-friction coefficients on a flat plate in high-speed flow. The postulates employed in the development of these analyses are discussed. New solutions are presented which show both the effect of using a continuous velocity gradient at the interface of the sublayer and the outer region of the boundary layer, and the effect of the extent of the laminar sublayer on the average skin-friction coefficient. From examination of the various analyses, the effect on the calculated skin-friction coefficient of using either the von Kármán or the Prandtl mixing length is determined. These effects are shown numerically as a function of Mach number for $Re = 7 \times 10^6$.

Average skin-friction coefficients on an insulated flat plate were measured at a Mach number of 2.5 and over a Reynolds number range of $2.1 \times 10^6 < Re < 6.2 \times 10^6$ and the data are compared with the several analyses. The analysis that corresponds most closely to the experimental data for average skin-friction coefficient is the extended Frankl and Voishel analysis, for which a convenient interpolation formula is presented for the case of an insulated flat plate. In addition, other experimental data for various Mach and Reynolds numbers were found to agree with the extended Frankl and Voishel analysis. The widely known von Kármán estimation formula gave values of average skin-friction coefficients that are 14.5 percent lower than the experimental data for $M_o = 2.5$.

From the Reynolds analogy between skin friction and heat transfer for a flat plate with constant surface temperature and for a Prandtl number equal to unity, the results obtained for the skin-friction coefficient hold equally well for the heat-transfer coefficient.

## INTRODUCTION

In many cases, skin-friction drag represents a significant portion of the total drag of a supersonic vehicle. The magnitude of the skin

friction, therefore, assumes considerable importance in the process of computing performance, particularly range. Because of the high speeds of these vehicles, the resulting frictional heating also makes a consideration of the heat transfer important, due to its effect on the structure and load.

The turbulent boundary layer is often the type of boundary layer occurring on these vehicles. Nevertheless, knowledge of the skin-friction and heat-transfer characteristics in turbulent boundary layers is meager when speeds are sufficiently high to introduce frictional heating and the accompanying variations through the boundary layer of density, viscosity, and thermal conductivity. The reason for this dearth of information is three-fold. First, exact analysis of the turbulent boundary layer is not possible at present because the mechanism of turbulence, even in the simplest cases, is not thoroughly understood. Second, an approach to a description of the real mechanism, such as the use of statistical methods, introduces such complex mathematics that the problem has so far proved to be intractable. Third, experimental investigation has been neglected somewhat because of the preoccupation of existing high-speed wind tunnels with aerodynamic problems such as over-all drag, lift, stability, etc.

A number of approximate analyses exist which allow computation of the coefficients of skin friction and heat transfer of a flat plate in supersonic flow. These flow conditions and plate temperatures would bring about variations in the fluid properties: density, viscosity, and thermal conductivity. It is the purpose of the analytical portion of this report to review these analyses and to investigate the effect of certain arbitrary boundary conditions which are imposed in the analyses. It is the purpose of the experimental portion of this report to present additional data on the high-speed, turbulent-boundary-layer, skin-friction characteristics and to compare these data and other data with the results given by all the theories.

## NOTATION

$a$ thermal diffusivity $\left(\frac{k}{\rho c_p g}\right)$, square feet per second

$c_f$ local skin-friction coefficient, dimensionless

$C_f$ average skin-friction coefficient $\left(\frac{1}{x}\int_0^x c_f \, dx\right)$, dimensionless

$c_p$ specific heat at constant pressure, Btu per pound, $^\circ F$

$g$ gravitation force per unit mass, 32.2 feet per second per second

$h$ average heat-transfer coefficient, Btu per second, square foot, $^{\circ}F$

$H$ boundary-layer-shape parameter, ratio of displacement thickness to momentum thickness, dimensionless

$k$ thermal conductivity, Btu per second, square foot, $^{\circ}F$ per foot

$K$ constant in von Kármán's similitude expression, dimensionless

$l$ mixing length, feet

$M$ Mach number, dimensionless

$Nu$ Nusselt number $\left(\frac{hx}{k}\right)$, dimensionless

$Pr$ Prandtl number $\left(\frac{\nu}{a}\right)$, dimensionless

$Pr_e$ effective Prandtl number $\left(\frac{\nu + \epsilon_H}{a + \epsilon_M}\right)$, dimensionless

$r$ temperature recovery factor, dimensionless

$Re$ Reynolds number $\left(\frac{u_o \rho_o x}{\mu_o}\right)$, dimensionless

$T$ temperature, $^{\circ}F$ absolute

$u$ velocity parallel to plate, feet per second

$u^+$ velocity parameter $\left[\frac{u}{u_o(c_f/2)^{1/2}}\right]$, dimensionless

$x$ distance along plate from leading edge, feet

$y$ distance normal to plate, feet

$y^+$ distance parameter $\left[\frac{y\, u_o \rho_o (c_f/2)^{1/2}}{\mu_o}\right]$, dimensionless

$\gamma$ ratio of specific heats (1.40, for air), dimensionless

$\delta$ boundary-layer thickness, feet

$\delta^*$ displacement thickness, feet

$\Delta x_e$ effective starting length $(x-x_e)$, inches

$\epsilon_H$ eddy diffusivity of heat (virtual thermal diffusivity resulting from the mechanism of turbulence), square feet per second

$\epsilon_M$ eddy diffusivity of momentum (virtual kinematic viscosity resulting from the mechanism of turbulence), square feet per second

$\theta$ momentum thickness, feet

$\mu$ viscosity, pound-second per square foot

$\nu$ kinematic viscosity $\left(\frac{\mu}{\rho}\right)$, square feet per second

$\rho$ mass density, slugs per cubic foot

$\tau$ local shear stress, pounds per square foot

$\omega$ temperature, absolute viscosity exponent $\left[\frac{\mu}{\mu_o} = \left(\frac{T}{T_o}\right)^{\omega}\right]$, dimensionless

Subscripts

a conditions at the interface of the laminar sublayer and the outer region of the boundary layer

e referring to an effective length

o free-stream conditions

w plate-surface conditions

## REVIEW OF ANALYSES

At present, there are a number of methods available for estimating the effect on the skin friction and heat transfer of the variation of density, viscosity, and thermal conductivity. The earliest and most widely known method was suggested by von Kármán, reference 1. In this method the skin-friction coefficient (and heat-transfer coefficient) is evaluated from low-speed relationships in terms of Reynolds number with the modification that the fluid properties used in these terms are no longer evaluated at the free-stream temperature but are replaced by the properties evaluated at the surface temperature. This is a first approximation to the problem and is based on the premise that the properties of the fluid next to the surface determine the skin friction. A result of this method, for example, is to predict a reduction in the coefficient of skin friction for an insulated surface in an air flow at a free-stream Mach number of 3 and $Re = 7 \times 10^6$ of about 50 percent

below its value for the $M = 0$, or constant property, case at the same free-stream Reynolds number.

The effect of variation of fluid properties through the boundary may also be obtained from several analyses. The methods of these analyses are similar, and the following is a resumé of the general method used.

## Method of Analyses

It is assumed that the portion of the boundary layer treated is sufficiently far from the leading edge of the plate that changes of variables in the $x$ direction are negligible compared to changes in the $y$ direction.

The boundary layer is divided into two regions. The first region is the laminar sublayer and is the region next to the surface in which molecular viscous forces are considered to predominate. The differential equation governing the velocity distribution in this layer is

$$\tau = \mu \frac{du}{dy} \tag{1}$$

The second region is comprised of that portion of the boundary layer outside of the laminar sublayer. In this region, in the most general form, both molecular viscous forces and eddying viscous forces are present. The equation for this region is postulated (reference 2) as

$$\tau = \mu \frac{du}{dy} + \rho l^2 \left(\frac{du}{dy}\right) \left|\frac{du}{dy}\right| \tag{2}$$

The second term of the right member of equation (2), representing the eddying shearing forces, is assumed to apply to a compressible gas when a variable density term is used. The assumption here is that the component of shear stress produced by the fluctuating density is small compared to the other terms.

Two forms of the mixing length expression $l$ may be used. For incompressible flow, Prandtl (reference 2) postulated that

$$l = Ky \tag{3}$$

From the theory of mechanical similitude for incompressible flow, von Kármán (reference 3) deduced an alternative expression for the mixing length

$$l = K \frac{du/dy}{d^2u/dy^2} \tag{4}$$

The symbol K, which represents an empirical constant, is assumed to be independent of Mach number, Reynolds number, and the plate surface temperature. Its value of 0.4 has been determined from experimental determinations of the velocity distribution for incompressible flow in the entrance sections of channels and in the downstream portions of pipes by Reichardt and by Nikuradse, respectively (references 4 and 5).

In order to integrate equation (2) it is necessary to know the shear stress $\tau$ as a function of $y$. The manner in which the shear stress varies through a compressible boundary layer is not known at present. Although it must certainly vary from its value $\tau_w$ at the surface of the plate to zero at the outer edge of the boundary layer, the shear stress $\tau$ is assumed constant through the boundary layer and equal to its value at the plate surface. This simplifies the mathematics of the analyses considerably. Further, it will be shown later that this assumption is justified somewhat by the fact that analyses, using constant gas properties and employing the same assumption, indicate values of the skin-friction coefficient that compare well with low-speed experimental results. This does not necessarily mean that the shear stress is constant across the boundary layer, but rather that the large stress near the outer edge of the boundary layer is somehow compensated by the high value of mixing length assumed near the outer edge of the boundary layer.

The values of the viscosity and density terms in equation (2) are obtained by relating the local temperature to the local velocity as indicated by Crocco (reference 6). This relationship results directly from the postulate that the effective Prandtl number is unity throughout the boundary layer. Further, it is implied that the energy of the turbulent fluctuations and the energy dissipation by these fluctuations are small in comparison with the corresponding characteristics of the mean flow.

To obtain particular solutions of equation (2), it is necessary to impose certain boundary conditions. When equation (3) is used for the mixing length, one boundary condition is required. When equation (4) is used, two boundary conditions are required. The number of boundary conditions are determined by the order of the differential equation resulting from the combination of equation (3) or (4) with equation (2). When equation (3) is used, the boundary condition imposed is the extent of the laminar sublayer, specified by the distance from the surface to the interface of the sublayer and the outer region of the boundary layer and by the velocity occurring at the interface. When equation (4) is used, in addition to the above boundary condition, it is necessary to impose the boundary condition of the velocity gradient occurring on the side of the interface in the outer region of the boundary layer. Since no experimental data exist which indicate the values of these boundary conditions in the high-speed boundary layer, it is necessary to base the extent of the sublayer and the velocity gradients at the interface on experimental values determined at low speeds. The data used to obtain these values are shown

in figure 1. In figure 1 is shown von Kármán's empirical curve representing the data for fully developed, turbulent velocity distributions in pipes and channels. The coordinate system of $u^+$ and $y^+$ used in this figure allows correlation of the constant property data. When it is postulated that the velocity in the sublayer varies linearly with the distance from the surface, the dotted curve shown in this figure is obtained. The conditions at the interface are given by the intersection of these lines. Thus, at the interface

$$u_a^+ = 11.5 \tag{5}$$

It is to be noted that a discontinuity in the velocity gradient occurs at this point; $du^+/dy^+$ varies from 1 in the sublayer to 0.218 in the outer region of the boundary layer, that is

$$\left(\frac{du^+}{dy^+}\right)_{a+} = 0.218 \tag{6}$$

In all the analyses, except where noted, these boundary conditions are modified somewhat arbitrarily to account for compressibility, and there results

$$u_a^+ = 11.5\left(\frac{T_w}{T_o}\right)^{1/2} \tag{7}$$

and

$$\left(\frac{du^+}{dy^+}\right)_{a+} = 0.218\left(\frac{T_o}{T_w}\right)^{\omega} \tag{8}$$

This is equivalent to stating that the interface acts as one in a fluid having constant properties evaluated at the surface temperature. An $\omega$ of unity was used in the numerical work of this report. The corresponding value of $y^+$ is found directly from integration of equation (1).

When these boundary conditions are imposed on the results obtained by integration of equation (2), the velocity distribution is obtained for a specified local skin-friction coefficient and specified thermal and flow conditions. When these velocity distributions, together with the local density, are introduced into the von Kármán momentum integral, which is

$$\tau = \frac{d}{dx}\int_o^\delta \frac{\rho u}{\rho_o u_o}\left(1 - \frac{u}{u_o}\right) dy$$

the Reynolds number at which the particular velocity distribution and skin friction occur is determined. Thus, a relationship between the skin-friction coefficient and Reynolds number is established.

The postulate that the effective Prandtl number is unity and the condition that a constant pressure exists along the plate allow application of the Reynolds analogy (reference 7) to relate the coefficients of heat transfer and skin friction; thus

$$Nu = \frac{C_f}{2} Re \tag{9}$$

## Particulars of Analyses

In 1937, Frankl and Voishel (references 8 and 9) performed the analysis indicated in the foregoing section. The eddy forces of equation (2) were considered to predominate and, consequently, the viscous portion of the stress was neglected. Equation (4) was used for the mixing length. Both boundary conditions (equations (7) and (8)) were employed. It should be noted, however, that the constant of equation (8) used in reference 8 was equal to 0.289. As the value 0.218 comes directly from the expression of von Kármán's empirical curve when $u_a^+ = 11.5$, some error is indicated in the report of Frankl and Voishel. Further, as the von Kármán momentum integral could not be solved in closed form, Frankl and Voishel performed this integration in terms of a power series in Mach number, thereby restricting the analysis to low free-stream Mach numbers. This analysis will be referred to, hereafter, as the original Frankl and Voishel analysis.

To avoid the restriction to low Mach numbers and to eliminate the apparent error in the constant of the boundary condition (equation (8)), the analysis was repeated herein, restricted to a linear variation of viscosity with temperature. The integration of the von Kármán momentum integral in this case was performed numerically. These computations, however, were restricted to an insulated plate (a plate with zero heat transfer at the surface). The average skin-friction coefficient on the insulated plate is given by the following interpolation formula which represents the results computed numerically to within ±2 percent in the range $0 < M_o < 4$:

$$C_f = \frac{0.472}{(\log_{10} Re)^{2.58} \left(1 + \frac{\gamma-1}{2} M_o^2\right)^{0.467}} \tag{10a}$$

The local skin-friction coefficient is given by the following interpolation formula:

$$c_f = \frac{0.472}{(\log_{10} Re)^{2.58} \left(1 + \frac{\gamma-1}{2} M_o^2\right)^{0.467}} \left(1 - \frac{1.12}{\log_{10} Re}\right) \tag{10b}$$

This analysis will be referred to, hereafter, as the extended Frankl and Voishel analysis. Another analysis along lines indicated previously was performed by Kalikhman in 1946 (reference 10). The molecular viscosity term of equation (2) was again omitted. Equation (3) was used for the mixing length, although it was modified somewhat so as to be linear in a new variable which defined the distance from the surface. The boundary condition represented by equation (7) was used. The significant results of the analysis happened to be identical with those of the method suggested by von Kármán, namely, use of wall properties in place of free-stream properties for the Reynolds number and the definition of the skin-friction coefficient.

The analysis by Ferrari in 1948 (reference 11), which also used the Prandtl mixing length expression, included the effect of the fluctuating density in addition to the variation of the mean density in the region outside the sublayer but neglected molecular viscosity. The results of this analysis are dependent on the value of a parameter introduced to account for the effect of the fluctuating density, the value of which is unknown initially. Ferrari indicated that the value of this parameter could be determined by comparing his analytical results with experimental data. The effect on skin friction and heat transfer of the variation of the fluid properties, therefore, cannot be determined from this analysis before knowledge of the parameter of density fluctuations is obtained from experiment.

The analysis made by Wilson in 1949 (reference 12) is the same as the original Frankl and Voishel analysis except in a few minor details. Wilson avoided the tedious numerical integration of the von Kármán momentum integral by using an interpolation expression which represented the integration to within 5 percent over a range of Mach numbers from 0 to 10. In deriving the Reynolds number expression, Wilson followed the procedure of von Kármán (reference 13) in dropping terms of lower order of magnitude which results in a simple expression for the average skin-friction coefficient in terms of Reynolds number and Mach number. This analysis, however, is restricted to the case of an insulated plate. The equation for determining the average skin-friction coefficient as given by Wilson is

$$\frac{\sin^{-1}\sqrt{\sigma}}{\sqrt{\sigma}}\left(1 + r\,\frac{\gamma-1}{2}\,M_o^2\right)^{-1/2}\frac{0.242}{\sqrt{C_f}} = \log_{10}(C_f \mathrm{Re}) - \omega \log_{10}\left(1+r\,\frac{\gamma-1}{2}\,M_o^2\right) \qquad (11)$$

where

$$\sigma = \frac{[(\gamma-1)/2]\ M_o^2}{1 + [(\gamma-1)/2]\ M_o^2}$$

The temperature recovery factor r was arbitrarily included in equation (11) by Wilson, although a Prandtl number of 1 was used throughout the development of the analysis.

Van Driest, in 1950, performed an analysis (reference 14) similar in procedure to the work done by von Kármán for the incompressible case (reference 13), except that the effect of compressibility was considered. Molecular viscosity was omitted in the region outside the sublayer and equation (3) was used for the mixing length. The boundary condition represented by equation (7) was used implicitly. Through the derivation of an interpolation expression for evaluating the von Kármán momentum integral, Van Driest obtained a simple expression for the skin-friction coefficient in terms of Reynolds number, Mach number, and, in addition, wall temperature, thereby including the effect of heat transfer.

The expression for the average skin-friction coefficient given by Van Driest is

$$\frac{0.242}{AC_f^{1/2}(T_w/T_o)^{1/2}} \left\{ \sin^{-1} \frac{[A-(B/2A)]}{[(B/2A)^2 + 1]^{1/2}} + \sin^{-1} \frac{(B/2A)}{[(B/2A)^2 + 1]^{1/2}} \right\} = \log_{10}(ReC_f) - \left(\frac{1+2\omega}{2}\right) \log_{10}\left(\frac{T_w}{T_o}\right) \quad (12)$$

where

$$A^2 = \frac{[(\gamma-1)/2]\ M_o^2}{T_w/T_o}$$

$$B = \left\{ \frac{1 + [(\gamma-1)/2]\ M_o^2}{T_w/T_o} \right\} - 1$$

## Effect of Boundary Conditions

It is believed that the two assumptions concerning the boundary conditions at the interface of the sublayer and the outer region of the boundary layer, represented by equations (7) and (8), are somewhat arbitrary. The first assumption (equation (7)) implies that the extent of the laminar sublayer is the same as in a fluid having constant properties evaluated at the surface temperature. This is based on reasoning similar to von Kármán's toward the relationships between the skin-friction coefficient and Reynolds number. The second assumption (equation (8)) states that the ratio of the velocity gradient in the outer region of the boundary layer to the velocity gradient in the sublayer is taken constant and equal to its value for the case of constant properties.

Although these assumptions are plausible, some test of their significance is necessary. For instance, if it is determined that a large change in these boundary conditions leaves the solutions unaffected, any differences between the results of analysis and experimental data can be attributed to some other quantity or postulate introduced into the analysis, as was done by Ferrari. If, however, the influence of these arbitrary boundary conditions is found to be large, little more than a possible range of theoretical results can be determined from analyses of this nature.

The effect of the first of these assumptions was determined by substituting equation (5) for equation (7), and repeating the extended Frankl and Voishel analysis. This made the extent of the sublayer identical to that in a fluid having constant properties which are evaluated at the free-stream temperature, the other extreme alternative. Integration of the von Kármán momentum integral was again performed numerically. In the following discussion the results of the computation are referred to as the modified Frankl and Voishel analysis.

The effect of the second assumption, concerning the velocity gradient at the interface, was determined by integrating the complete equation (2) and allowing the velocity gradient at the interface to be equal to the velocity gradient in the sublayer. In addition to allowing the velocity gradient to be continuous, this procedure introduced the effect of a buffer layer, the region between the completely laminar and completely turbulent regions, which is known to exist from experiments at subsonic speeds. The extent of the sublayer used in this analysis was

$$u_a^+ = 9 \tag{13}$$

which is in the same form as that of the modified Frankl and Voishel solution in that it does not include the variation of properties. The reason that equation (5) was modified can be seen by considering the

solid line in figure 1 which represents the velocity distribution for an incompressible fluid resulting from this analysis. It was necessary to alter the extent of the sublayer to the value given by equation (13) so that the velocity distribution approached the fully turbulent velocity distribution asymptotically near the outer edge of the boundary layer. All integrations in this method were performed numerically for $\omega = 1$. In the following, the results of the analysis are referred to as the buffer-layer analysis.

## Comparison of Analytical Methods

For the $M = 0$ case, the Frankl and Voishel and the buffer-layer analyses reduce to Schlichting's interpolation equation for incompressible flow (reference 15), which is

$$C_f = \frac{0.472}{(\log_{10} Re)^{2.58}} \tag{14}$$

It is interesting that the results of the Frankl and Voishel analysis and the buffer-layer analysis are essentially the same for $M = 0$, indicating that both the slightly different extent of the sublayer and molecular viscosity in the outer region of the boundary layer have little effect on the average skin-friction coefficient, at the Reynolds numbers indicated, when the fluid properties are constant. Van Driest's and Wilson's analyses at $M = 0$ reduce to von Kármán's empirical drag law for incompressible flow, that is,

$$\frac{0.242}{\sqrt{C_f}} = \log_{10} (C_f Re) \tag{15}$$

A comparison of these equations with existing data is made in figure 2.

In figure 2, the results of equation (14) are shown to be about 4 percent higher than the values given by equation (15) which is based on the data of Kempf (reference 15). The data of Wieselsberger (reference 15) are slightly higher than these results.

In figure 3, a comparison of the local skin-friction coefficient determined from the interpolation formula of the extended Frankl and Voishel analysis (equation (10a)) is compared with the local skin-friction coefficient calculated from the original Frankl and Voishel analysis (equation (8) of reference 9). The ratio of the local skin-friction coefficient for compressible flow to the local skin-friction coefficient for incompressible flow is plotted against Mach number. As can be seen from figure 3, using the power series for the solution of the momentum integral, as was done in the original Frankl and Voishel

analysis, rather than using the less restricted numerical solution, as was done in the extended Frankl and Voishel analysis, introduces a deviation in the local skin-friction coefficient that increases with increasing Mach number. At $M = 3$, for example, this deviation is of the order of 12 percent. These conclusions are essentially independent of the value of the constant of the boundary condition (equation (8)).

A comparison of the several analyses up to a Mach number of 4 is shown in figure 4 for an insulated plate at a Reynolds number of $7 \times 10^6$. The ratio of the average skin-friction coefficient for compressible flow to the average skin-friction coefficient for incompressible flow is plotted against Mach number for the various analyses. The analyses presented are the Frankl and Voishel modified, the buffer-layer, the Van Driest, the Wilson, the extended Frankl and Voishel, and the von Kármán estimation applied to equation (14).

For a Mach number of 3, the percentage reduction of average skin-friction coefficient from the $M = 0$ case of each of the analyses is given below:

| | |
|---|---|
| Modified Frankl and Voishel | 7 percent |
| Buffer-layer | 17.5 percent |
| Van Driest | 27 percent |
| Wilson | 34 percent |
| Extended Frankl and Voishel | 38 percent |
| von Karman's estimation | 49 percent |

For sake of comparison in figure 4, unity was used for both the recovery factor and for $\omega$, the exponent in the viscosity-temperature variation, in all the analytical methods.[1]

Comparison of the modified and extended Frankl and Voishel methods indicates that the extent of the sublayer alters the skin-friction drag by 31 percent for the $M_o = 3$ case. Thus, using the wall properties of the fluid to govern the thickness of the sublayer is arbitrary, although plausible. It is apparent that the choice of temperature used in the

[1]After completion of the work presented in this report, a new theory by Eckert for determining skin-friction coefficients along a flat plate was published in the Journal of Aeronautical Sciences, volume 17, number 9, September 1950. Eckert developed a theory for flow in pipes which correlates experimental data from supersonic flow in pipes. He then transformed this empirical theory for pipe flow to flow along a flat plate and obtained a relationship for calculating skin-friction coefficients along a flat plate. The calculated results of this empirical theory would lie between the buffer-layer analysis and Van Driest's analysis if Eckert's results were plotted in figure 4.

evaluation of the fluid properties has a very large effect on the skin-friction coefficient. If the fluid properties were evaluated at the wall temperature in the buffer-layer analysis, the skin-friction coefficients obtained would be the same as from von Kármán's estimation.

Comparison of the modified Frankl and Voishel and the buffer-layer analyses shows the effect of using a continuous velocity gradient at the interface of the sublayer and the outer region of the boundary layer, and the effect of adding the molecular viscosity term in the expression for the shear in the outer region of the boundary layer. This combined effect lowers the skin-friction coefficient from the modified Frankl and Voishel analysis by 10.5 percent for the $M_o = 3$ case.

Comparison of the Wilson and the extended Frankl and Voishel analyses shows the relative accuracy of both neglecting terms of lower order of magnitude in the expression for the velocity distribution and using an approximate interpolation formula for von Kármán's momentum integral. These factors caused the average skin-friction coefficient (at $M_o = 3$) of the Wilson analysis to be 4 percent higher than the extended Frankl and Voishel analysis.

Comparison of the Wilson and the Van Driest solutions for the case of the insulated plate shows the effect of the use of different mixing lengths in the shear expression, that is, equations (4) and (3), respectively. Van Driest and Wilson make similar mathematical approximations in order to integrate the von Kármán momentum integral. The net result of these differences for the insulated plate is that the final equations of average skin-friction coefficient and Reynolds number differ only by a factor of 1.5 in the constant term when $\omega = 1$. For the $M_o = 3$ case of the insulated plate, the average skin-friction coefficient from Van Driest's analysis is 7 percent higher than the values from the Wilson analysis.

The von Kármán estimation method applied to Schlichting's equation for incompressible flow shows the greatest reduction of average skin-friction coefficient from the $M = 0$ to the $M_o = 3$ case, that is, 49 percent.

In view of the wide difference in the predicted skin-friction variation with Mach number resulting from the several analyses, each of which is based on a more or less arbitrary set of assumptions, it is necessary to compare the results of these analyses with the results of experimental data to establish which of the basic postulates best predicts skin-friction coefficients.

## REVIEW OF PREVIOUS EXPERIMENTAL RESULTS

Two sets of experiments are known to have been conducted to determine skin-friction coefficients on an insulated flat plate at supersonic speeds.

One set of data was obtained by Wilson, Young, and Thompson (reference 16). The data were taken over a range of Mach numbers from 1.60 to 2.19 and a range of Reynolds numbers from about $4.4 \times 10^6$ to about $19 \times 10^6$. Since natural transition from a laminar to a turbulent boundary layer occurred far from the leading edge, the total skin-friction measured included a considerable laminar and transitional portion at Mach numbers above 1.9 but not at the lower Mach numbers. By assuming the boundary layer to have a 1/7-power-law velocity distribution in the region beyond a transition point, Wilson, Young, and Thompson were able to transform their data at the higher Mach numbers to a Reynolds number based on an effective length of the fully turbulent boundary layer. This method restricted the form of the skin-friction data so that it varied with the 1/5 power of the effective Reynolds number, even though this variation actually may not have existed. Thus, the method of interpretation is somewhat in doubt at the higher Mach numbers.

Realizing these limitations, Wilson reinterpreted these and some additional data according to his afore-mentioned theory (reference 12), again subjecting the results at the higher Mach numbers to a possible restriction. For the range of Mach numbers and Reynolds numbers tested, the agreement between the experimental results and theory was within a maximum deviation of 7 percent.

The following portions of the present report describe experiments carried out at Ames Laboratory to provide additional data at higher Mach numbers for comparison with the data just discussed, and with the results given by all the theories.

## DESCRIPTION OF EQUIPMENT

### Ames 6-Inch Heat-Transfer Tunnel

The 6-inch heat-transfer tunnel used in the present study has been described in detail in reference 17.

## The Flat Plate Model

The full-span flat-plate model used for the tests, shown schematically in figure 5, was constructed from stainless steel. The model was 16 inches long, approximately 5-1/2 inches wide, and 1/2 inch thick. The leading edge was chamfered to form an angle of 15°, and was rounded to a radius of about 0.003 inch. The top surface of the plate was ground and polished. Static-pressure orifices, 0.0135 inch in diameter, were placed in a line 1 inch from each side of the plate (fig. 5). A strip of lampblack extending from the leading edge to 1/2 inch from the leading edge was used to cause transition of the boundary layer from laminar to turbulent flow. Clear lacquer was sprayed on the model and the lampblack was dusted on to form the boundary-layer trip. The region from 4 inches to 8 inches from the leading edge constituted the testing region.

The support for the flat-plate model consisted of a steel plate, 3/4 inch thick, which was bolted to the rear portion of the test plate. The supporting plate was secured to removable side plates in the tunnel walls downstream from the testing section. Both the test plate and the supporting plate spanned the test section and were sealed at the walls.

## Boundary-Layer Survey Apparatus

The impact-pressure probe (see fig. 5) used in the boundary-layer surveys was made of 0.063-inch stainless-steel tubing and had a rectangular opening 0.080-inch by 0.013-inch outside dimensions and 0.075-inch by 0.008-inch inside dimensions. With the probe in contact with the plate, the center line of the probe was 0.0065 inch above the plate surface. Stainless-steel stiffeners were soldered to the probe to prevent its deflection by the air stream (fig. 5).

The probe used for the static-pressure survey was made of 0.100-inch outside-diameter stainless-steel tubing and had an ogival head with four equally spaced orifices 0.0135 inch in diameter located at a cross section 0.79 inch from the tip.

The height of the impact-pressure probe above the surface of the plate was measured by visual observations with a cathetometer. To eliminate refraction errors due to density gradients in the boundary layer, fine lines were scribed high enough on the body of the probe to be in the free stream at all times, and the cathetometer was focused on the lines rather than on the tip of the probe itself.

## TEST PROCEDURE

### Method of Obtaining Data

The test conditions for the flat-plate model were chosen so as to obtain the largest possible range of Reynolds numbers based on the length along the plate and to obtain a turbulent boundary layer with a minimum of disturbances from the boundary-layer trip as indicated by mean velocity distributions. With the lampblack boundary-layer trip it was necessary to start testing at 4 inches from the leading edge of the model to be out of the region affected by the wake from the trip. The maximum length along the plate that could be used for testing was limited to 8 inches by both the travel of the traversing mechanism and the reflected bow shock wave.

The actual testing procedure was divided into the following phases:

1. A static-pressure survey was made with the static-pressure probe along the plate center line at 1-inch increments over the testing region of 4 to 8 inches at 30 to 40 pounds per square inch absolute stagnation pressures. This static-pressure probe was first calibrated by making surveys over the static-pressure orifices in the plate (fig. 5). Since a small static-pressure gradient was in evidence spanwise across the 5-1/2-inch tunnel width and the drag measurements were to be made along the center of the tunnel, it was decided to survey along the tunnel center line 1/2 inch above the plate with the static-pressure probe rather than use the values of static pressure obtained from the orifices in the plate.

2. With the lampblack boundary-layer trip existing from the leading edge to 1/2 inch from the leading edge, boundary-layer surveys were made at 1-inch increments over the 4-inch testing region at 30 and 40 psia stagnation pressures. The boundary-layer probe (fig. 5) was used in determining the impact pressures.

The impact, static, and stagnation pressures were measured with a mercury manometer with a high vacuum system as a reference. The reference pressures were measured with a McLeod gage.

In making the boundary-layer surveys with the impact-pressure probe, the cathetometer readings could be repeated to within ±0.001 inch. The zero distance of the probe above the plate was determined by visual means. Various methods were tried earlier for setting this zero point. Electrical contact of the probe with the plate surface and the impact-pressure minimum methods were used. It was found that the zero point could be obtained with the same accuracy by visual means as by either of the above methods, and to do so was much more convenient.

The time lag of the probe was of the order of 2 minutes. Chances of error due to time lag were minimized by waiting 4 minutes between each reading and by traversing up through the boundary layer and then back down to the plate surface for each survey.

## Reduction of Data

The momentum thickness from von Kármán's momentum integral is given by

$$\theta = \int_0^{\delta} \frac{\rho u}{\rho_0 u_0} \left(1 - \frac{u}{u_0}\right) dy \tag{16}$$

This equation can be expressed in terms of local Mach number in the boundary layer by using a temperature distribution as in reference 6 for a turbulent boundary layer,

$$\theta = \frac{1}{M_0^2} \int_0^{\delta} \left[ M M_0 \left( \frac{5+M^2}{5+M_0^2} \right)^{1/2} - M^2 \right] dy \tag{17}$$

The momentum thickness was calculated for each test condition by integrating equation (17) numerically using Simpson's rule.

The displacement thickness in terms of local density and local velocity is given by

$$\delta^* = \int_0^{\delta} \left(1 - \frac{\rho u}{\rho_0 u_0}\right) dy \tag{18}$$

The displacement thickness can be expressed in terms of local Mach number in the same manner as the momentum thickness,

$$\delta^* = \int_0^{\delta} \left[ 1 - \frac{M}{M_0} \left( \frac{5+M^2}{5+M_0^2} \right)^{1/2} \right] dy \tag{19}$$

The displacement thickness was calculated for each test condition by integrating equation (19) numerically using Simpson's rule.

Since turbulence in the boundary layer was artificially induced by means of a lampblack boundary-layer trip at the leading edge of the plate, the combined effects of the form drag as well as the shock waves from the bow of the plate and trailing edge of the lampblack made it meaningless to use the length from the leading edge of the plate as the

characteristic length of the turbulent boundary layer. Therefore, a method was devised for determining the effective length for the fully developed turbulent boundary layer.

The starting point of the effective length was determined in the following manner: All the theories predict that $\theta$, the momentum thickness, varies in a given range of Reynolds number with some power of the effective length of the turbulent boundary layer. This exponent of the effective length ranges from 0.804 to 0.832 for all the theories in the range of Reynolds numbers tested. The original data were plotted on logarithmic graph paper against the actual distance along the plate. The slope $d(\log 2\ \theta)/d(\log x)$ was determined by the method of least squares. Each point was then altered in $x$ by an equal amount until a value of the slope was obtained which was equal to the mean slope of the analytical methods having the extreme slopes. This mean slope is equal to 0.818. The equal amount by which each point was altered in $x$ to give a value of the slope equal to the mean slope of the theories was then taken to be the length by which the plate was altered to produce an effective plate length.

Figure 6 shows the procedure as applied to the data obtained at 40 psia stagnation pressure. The original data are shown plotted with circular points, and the slope as determined by the method of least squares is 0.670. To each $x$ distance of the data points 1.35 inches was then added and these adjusted points were plotted as shown by the square points. The slope of this line is 0.818 and, since this slope is the same as the average slope of the theories having the extreme slopes, the effective leading edge was 1.35 inches upstream of the actual leading edge of the plate. This procedure was repeated for the data from the 30 psia stagnation pressure tests, and the effective starting point based on the mean slope of the theories was found to be 1.30 inches upstream of the leading edge. These effective starting lengths were used to determine the characteristic dimension $x$ used in evaluating the average skin-friction coefficient and the Reynolds number.[2]

[2]As a check on the method of determining the effective starting length of the turbulent boundary layer, this method was applied to a limited set of data obtained using a 0.012-inch wire as a turbulence promoter. The effective starting length was determined in the afore-mentioned manner and found to be 0.2 inch upstream of the leading edge of the plate. The average skin-friction coefficient determined from the tests with the wire turbulence promoter (effective starting length 0.2 inch) agreed within the accuracy of the experiments with the corresponding results obtained with the lampblack turbulence promoter (effective starting length 1.35 inches), thus providing additional evidence for justifying the method of determining effective starting length.

## Discussion of Experimental Errors

The possible error in the experimental skin-friction coefficients contributed by reading of the instruments was of the order of ±2.5 percent.

A maximum variation of 2 percent in free-stream Mach number existed along the testing region (fig. 7). The effect of this slight Mach number variation on the average skin friction was calculated using von Kármán's boundary-layer momentum equations in integral form, and found to be less than 2 percent of the value of the skin friction determined when neglecting the Mach number gradient.

The velocities used in determining the average skin-friction coefficients were computed on the assumption that the energy per unit mass in the boundary layer was constant. Wilson, Young, and Thompson (reference 16) have shown that this assumption gives an error in the velocity of less than 1-1/2 percent at a Mach number of 2.

Tests were conducted to determine whether the velocity gradient across the opening of an impact-pressure probe caused an error in assuming that the pressure measured existed at the geometric center of the probe. The dimensions of the rectangular opening of the probes tested were 0.001-, 0.002-, 0.004-, and 0.006-inch inside heights, and 0.003-, 0.006-, 0.008-, and 0.013-inch outside heights, respectively. The inside width of all the probes was 0.065 inch with an outside width of 0.080 inch. When the geometric center of the probes was used to determine the distance from the surface of the plate, the results of the tests indicated that the probe size had no effect on the impact-pressure measurements within the experimental accuracy of the tests. These results were corroborated by Wilson and Young (reference 18).

Other possible sources of error are the unknown effect of the finite thickness of the model leading edge on the boundary layer, the influence of the bow wave off the leading edge of the plate, and the influence of the shock wave and expansion wave off the lampblack boundary-layer trip. These effects would contribute an error in the measured skin-friction coefficients which is believed to be eliminated by determining an effective starting length as described in the reduction of data.

Mach number profiles in the boundary layer obtained at several spanwise positions and visual observations of boundary-layer transition by luminescent lacquer techniques have indicated that the effects of transverse contamination in the testing region were small and were confined to the regions close to the walls.

## DISCUSSION OF RESULTS

In table I are shown the experimentally determined values of the momentum thickness, the displacement thickness, and the shape parameter determined from numerical integration of the boundary-layer velocity distributions. Values of momentum thickness indicated are those used in evaluating the average skin-friction coefficient in the portions of the report which follow.

The velocity distribution in the boundary layer of the flat plate is shown in figure 8. Each of the impact-pressure probe surveys is plotted in terms of $u/u_o$ versus $y/\theta$. Figure 8 indicates that the boundary layer for each axial position and stagnation pressure level was essentially of the same shape, and that throughout the region tested the boundary layer was fully turbulent.

When the effective starting points for a fully developed turbulent boundary layer were determined as explained in the reduction of data, it was possible to evaluate the average skin-friction coefficient and the Reynolds number based on the effective length of the fully turbulent boundary layer (from the values of $\theta$ taken from table I). These are plotted in figure 9. As the exponent of $x$ used in the relationship between $\theta$ and $x$ corresponds to the mean of the theories, it is possible, therefore, to compare the corresponding skin-friction coefficients with all the theories. For this comparison, all the aforementioned theories were evaluated for an insulated plate at a Mach number of 2.5. The exponent for the viscosity variation with temperature was set equal to unity in all these analyses because this value of the exponent is known to conform approximately to the experimental value of the viscosity exponent which was 0.87 in the range of temperatures experienced in the wind tunnel. In addition, Wilson's theory was evaluated using a recovery factor of 0.88 to determine the surface temperature of the plate. This procedure was recommended by Wilson although this contradicts his earlier postulate that Prandtl number is unity.

The data indicate that the extended Frankl and Voishel theory predicts the average skin-friction coefficient better than any of the other theories in the range of Reynolds numbers and at the Mach number tested. Because of this good agreement between the extended Frankl and Voishel analysis and the experiment, it was decided to again evaluate the effective starting point of the fully turbulent boundary layer, but this time to use the relationship between $\theta$ and $x$ for the extended Frankl and Voishel analysis $[d(\log 2\theta)/d(\log x) = 0.832]$ rather than the average of the theories.

The effective starting lengths determined from the slope of the extended Frankl and Voishel analysis were obtained as in figure 6. These lengths were 1.40 inches and 1.45 inches, ahead of the leading edge of the plate, for the 30 and 40 psia stagnation pressures, respectively. This changes the effective starting lengths from the previously determined values by 0.1 inch for each stagnation pressure.

The final data are presented in figure 10 using these new effective starting lengths to determine the final average skin-friction coefficient and effective Reynolds number. These data are compared with the extended Frankl and Voishel theory for a Mach number of 2.5, and the agreement is excellent.

As an additional check on the validity of the extended Frankl and Voishel analysis, all the available experimental data are compared with this analysis in figure 11. It can be seen from equations (10) and (14) that the ratio of the compressible to the incompressible average skin-friction coefficient is independent of Reynolds number and a function only of Mach number.

The two experimental points from the Ames 6-inch heat-transfer tunnel are arithmetic averages of five experimental points at each of the 30 and 40 psia stagnation pressure levels. The experimental points of Wilson (reference 12) representing seven different Mach numbers are arithmetic averages of five or six data points for each Mach number. For the incompressible experimental data, the one point from Kempf (reference 15) was an arithmetic average of nine experimental points and the one point from Wieselsberger (reference 15) represented an arithmetic average of fifteen experimental data points. The agreement between the available experimental data and the extended analysis of Frankl and Voishel is excellent over the range of Mach numbers $0 > M_o > 2.5$. It is of particular interest to note, however, that the experimental scatter of the incompressible data is greater than the scatter of the data at higher Mach numbers. Further, this agreement, by several experiments, indicates that the inherent errors in each of the experiments are either small or consistent.

Wilson (reference 12) corrected his data to account for the effective starting length of the turbulent boundary layer. These corrections altered the values of the skin-friction coefficients from 10 to 500 percent. Use of the effective starting length from the lampblack turbulence promoter in this report altered the skin-friction coefficients from 16 to 36 percent. From the limited data with the wire turbulence promoter, in this report, use of the effective starting length altered the skin-friction coefficients from 2.5 to 4 percent. With these corrections for the effective starting length of the turbulent boundary layer, the corrected data agreed with the theory of the extended Frankl and Voishel analysis to within ±5 percent.

A comparison of a typical experimental velocity distribution and a calculated velocity distribution from the Frankl and Voishel extended analysis is presented in figure 12. The ratio of the distance normal to the flat plate to the momentum thickness is plotted against the ratio of the local velocity in the boundary layer to the free-stream velocity. It was expedient to use the local skin-friction coefficients from the experimental data to determine the velocity distribution from the Frankl and Voishel analysis. The agreement between the experimental profile and the theoretical profile was not as close as might be expected from the excellent agreement of the experimental average skin friction with the Frankl and Voishel analysis. This might indicate that, although the skin-friction coefficient agrees with the theory very well, this agreement may be fortuitous since the velocity profiles are not coincident. This was also evident from the data of Wilson, as is pointed out in reference 12. The same condition is known to prevail at low Mach numbers. The difference between the theoretical and experimental velocity distributions is much larger than the possible error introduced by evaluating the experimental velocity distribution under the assumption of a constant energy per unit mass (references 6 and 16).

## CONCLUSIONS

The following conclusions can be drawn from the results of the present investigation:

1. A critical review of various analyses concerned with the prediction of skin friction on a flat plate with a compressible turbulent boundary layer has revealed that extremely large variations in the predicted average coefficients result from the differences in assumed mathematical boundary conditions.

2. An interpolation formula for the average skin-friction coefficient determined from the extended Frankl and Voishel analysis for an insulated flat plate agreed with previous and present experimental data to within ±5 percent in the range of Mach numbers, $0 < M_0 < 2.5$.

3. A comparison of a typical experimental boundary-layer velocity distribution with a theoretical velocity distribution based on the extended Frankl and Voishel analysis revealed that the profiles were not coincident. This indicates that the excellent agreement of the experimental average skin-friction coefficient with theory may be fortuitous.

Ames Aeronautical Laboratory,
National Advisory Committee for Aeronautics,
Moffett Field, Calif., October 25, 1950.

## REFERENCES


1. von Kármán, Th.: The Problem of Resistance in Compressible Fluids. Reale Accademia D'Italia, Roma. (Paper read at the 5th Volta Congress at Rome, Sept. 30 – Oct. 6, 1935.)

2. Prandtl, L.: Verhandlungen des 2. internationalen Kongresses für technische Mechanik, Zürich, 1926, pp. 62–74.

3. von Kármán, Th.: Mechanical Similitude and Turbulence. NACA TM 611, 1931.

4. Reichardt, H.: Heat Transfer through Turbulent Friction Layers. NACA TM 1047, 1943.

5. Nikuradse, J.: Geselzmassigkeiten der turbulenten Stromung in glatten Rohren. VDI, Forschungscheft, 356, 1932.

6. Crocco, L.: Transmission of Heat from a Flat Plate to a Fluid Flowing at High Velocity. NACA TM 690, 1932.

7. Goldstein, S. (Editor): Modern Developments in Fluid Dynamics. Oxford, The Clarendon Press, 1938, pp. 649–654.

8. Frankl, F.: Heat Transfer in the Turbulent Boundary Layer of a Compressible Gas at High Speeds,
and
Frankl, F., and Voishel, V.: Friction in the Turbulent Boundary Layer of a Compressible Gas at High Speeds. NACA TM 1032, 1942.

9. Frankl, F., and Voishel, V.: Turbulent Friction in the Boundary Layer of a Flat Plate in a Two-Dimensional Compressible Flow at High Speeds. NACA TM 1053, 1943.

10. Kalikman, L. E.: Heat Transmission in the Boundary Layer. NACA TM 1229, 1949.

11. Ferrari, Carlo: Study of the Boundary Layer at Supersonic Speeds in Turbulent Flow. Case of Flow Along a Flat Plate. Cornell Aeronautical Lab., CM 507, November 1, 1948.

12. Wilson, R. E.: Turbulent Boundary Layer Characteristics at Supersonic Speeds – Theory and Experiment. Univ. of Texas, Defense Research Lab., CM 569, November 21, 1949.

13. von Kármán, Th.: Mechanische Ahnlichkeit und Turbulenz. Proceedings of the 3rd International Congress for Applied Mechanics, pp. 85–89, August 1930.

14. Van Driest, E. R.: The Turbulent Boundary Layer for Compressible Fluids on a Flat Plate with Heat Transfer. North American Aviation, Aerophysics Lab., AL-1006, February 20, 1950.

15. Schlichting, H.: Lecture Series "Boundary Layer Theory" Part II - Turbulent Flows. NACA TM 1218, 1949.

16. Wilson, R. E., Young, E. C., and Thompson, M. J.: 2nd Interim Report on Experimentally Determined Turbulent Boundary Layer Characteristics at Supersonic Speeds. Univ. of Texas, Defense Research Lab., UT/DRL 196. January 25, 1949.

17. Stalder, J. R., Rubesin, M. W., and Tendeland, T.: A Determination of the Laminar-, Transitional-, and Turbulent-Boundary-Layer Temperature-Recovery Factors on a Flat Plate in Supersonic Flow. NACA TN 2077, 1950.

18. Wilson, R. E., and Young, E. C.: Aerodynamic Interference of Pitot Tubes in a Turbulent Boundary Layer at Supersonic Speed. Univ. of Texas, Defense Research Lab., CF 1351, December 6, 1949.

TABLE I.– MOMENTUM THICKNESS, DISPLACEMENT THICKNESS, AND SHAPE PARAMETER ALONG A FLAT PLATE, $M_o$ = 2.5.

| x in inches along plate | Nominal stagnation pressure (lb/sq in. absolute) | | | | | |
|---|---|---|---|---|---|---|
| | 30 | | | 40 | | |
| | $\theta \times 10^3$ in. | $\delta^* \times 10^3$ in. | H | $\theta \times 10^3$ in. | $\delta^* \times 10^3$ in. | H |
| 4 | 6.66 | 29.4 | 4.41 | 6.81 | 29.7 | 4.37 |
| 5 | 8.40 | 35.6 | 4.24 | 8.10 | 34.9 | 4.31 |
| 6 | 9.30 | 39.3 | 4.23 | 8.88 | 37.9 | 4.27 |
| 7 | 10.2 | 42.4 | 4.15 | 10.1 | 42.3 | 4.20 |
| 8 | 11.3 | 45.7 | 4.03 | 10.8 | 44.9 | 4.15 |

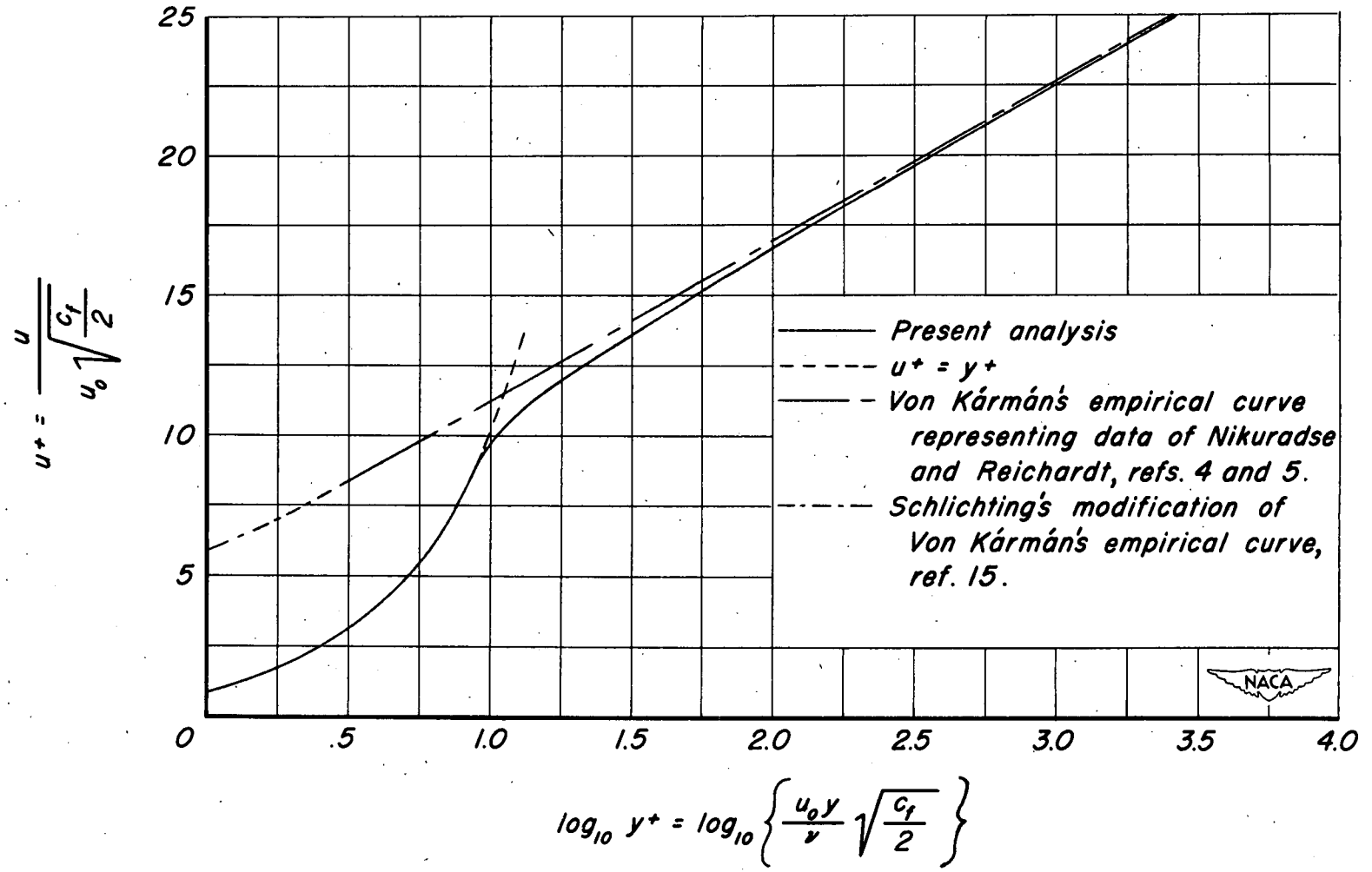


*Figure 1.-Comparison of velocity distributions for various constant property solutions.*

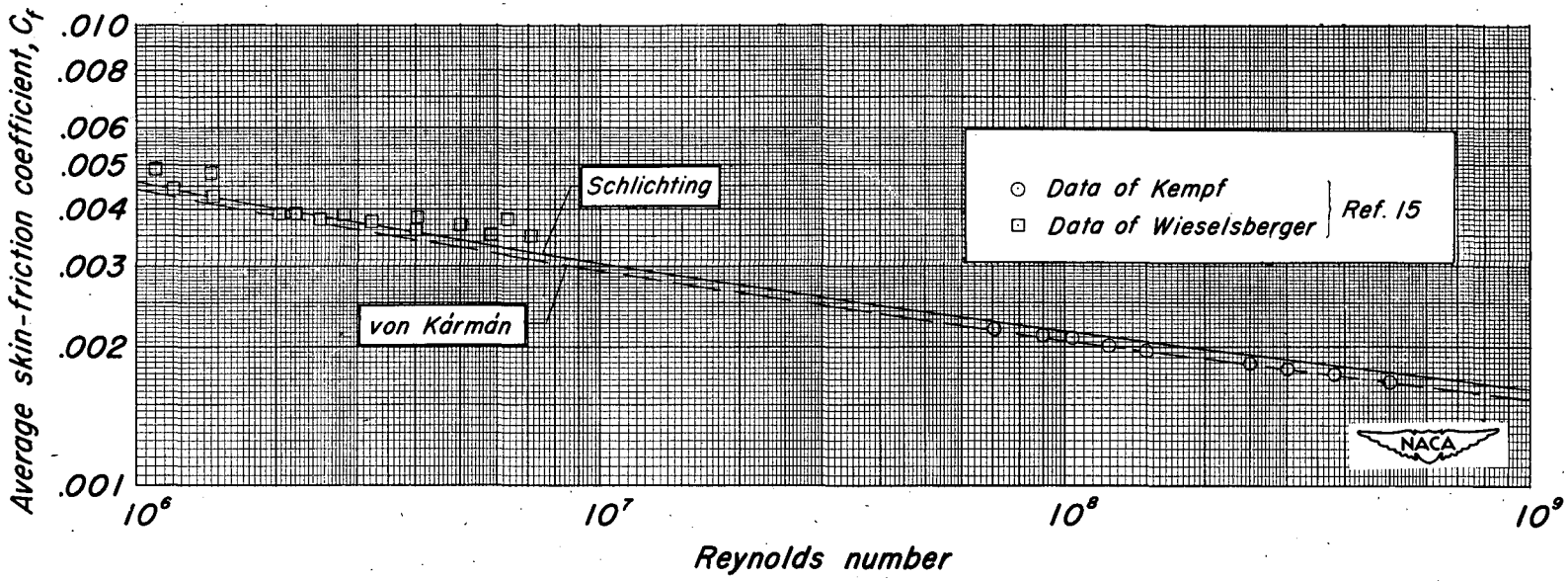


*Figure 2.- Comparison of average skin-friction coefficient evaluated for constant fluid properties.*

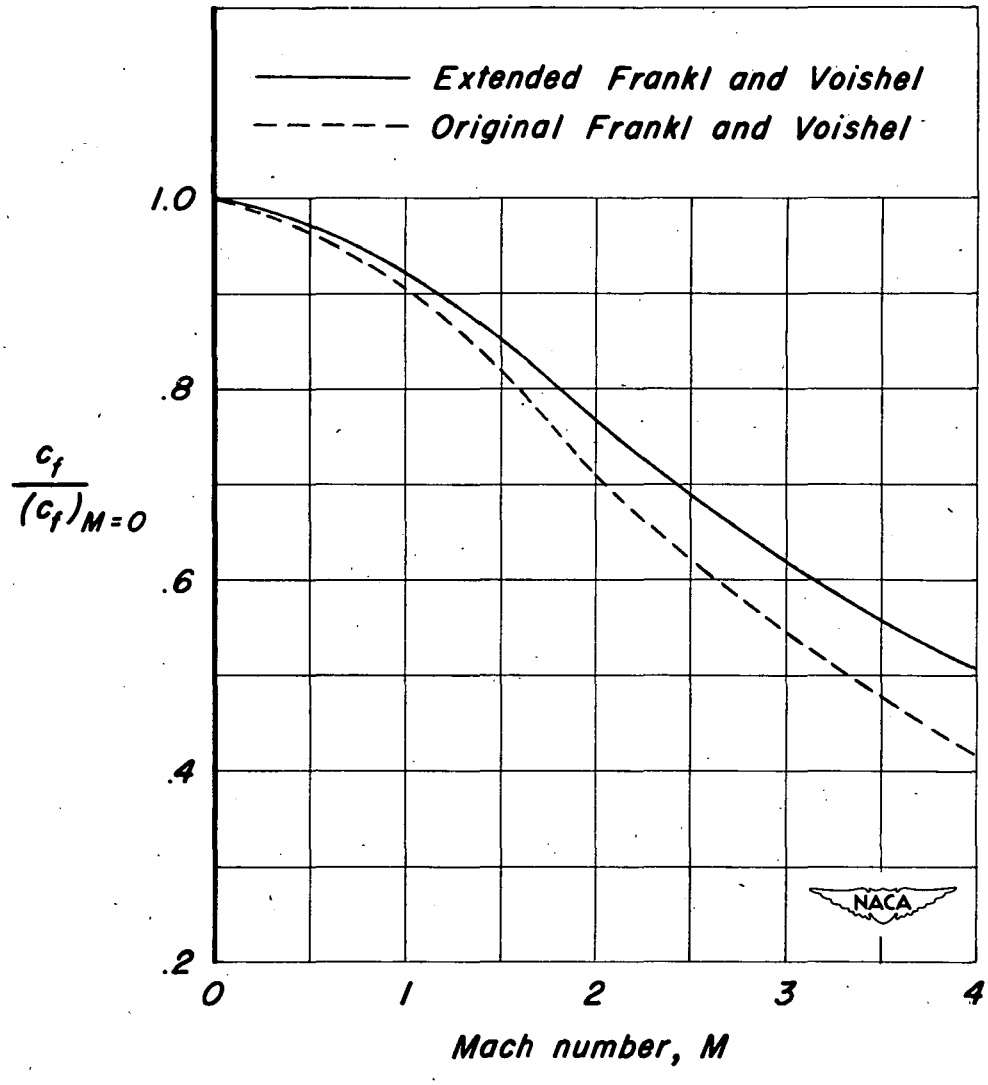


*Figure 3.- Comparison of the variation with Mach number of the local skin-friction coefficients determined from the extended Frankl and Voishel analysis and the original Frankl and Voishel analysis for an insulated flat plate at Re = $7 \times 10^6$.*

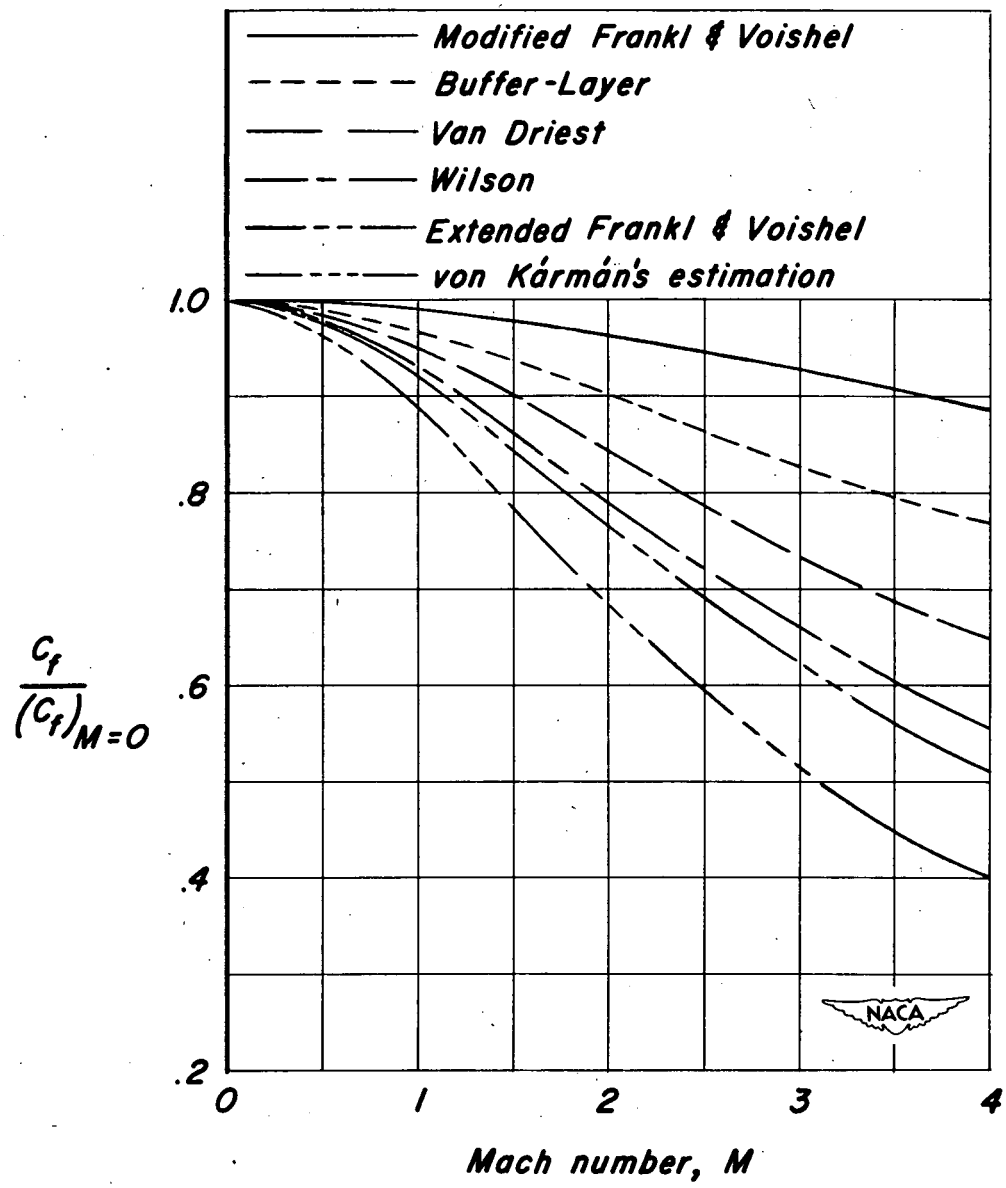


Figure 4.- Comparison of the variation with Mach number of the average skin-friction coefficients determined from the various analyses for an insulated plate at $Re = 7 \times 10^6$.

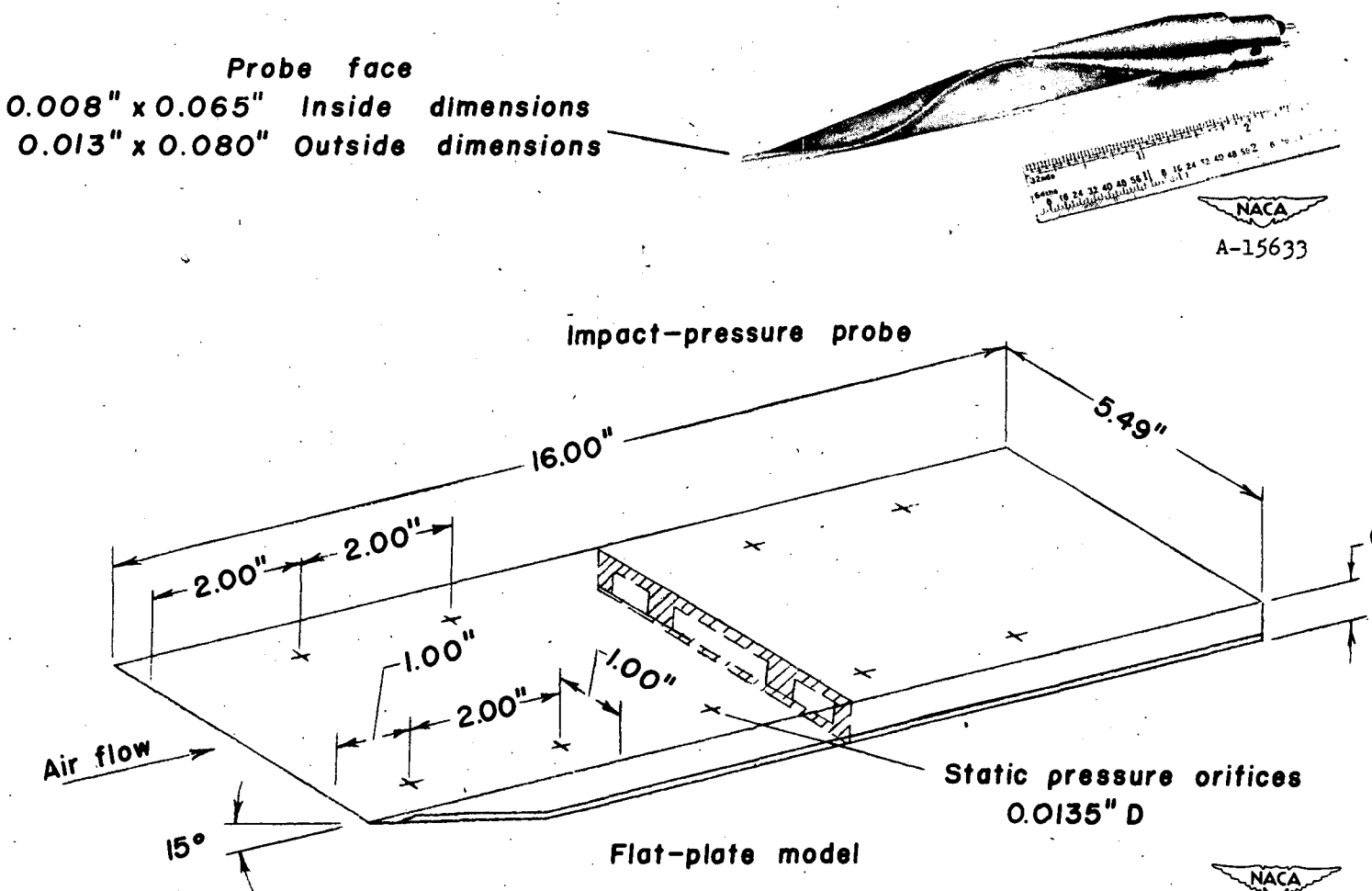


Figure 5. Flat-plate model and impact-pressure probe.

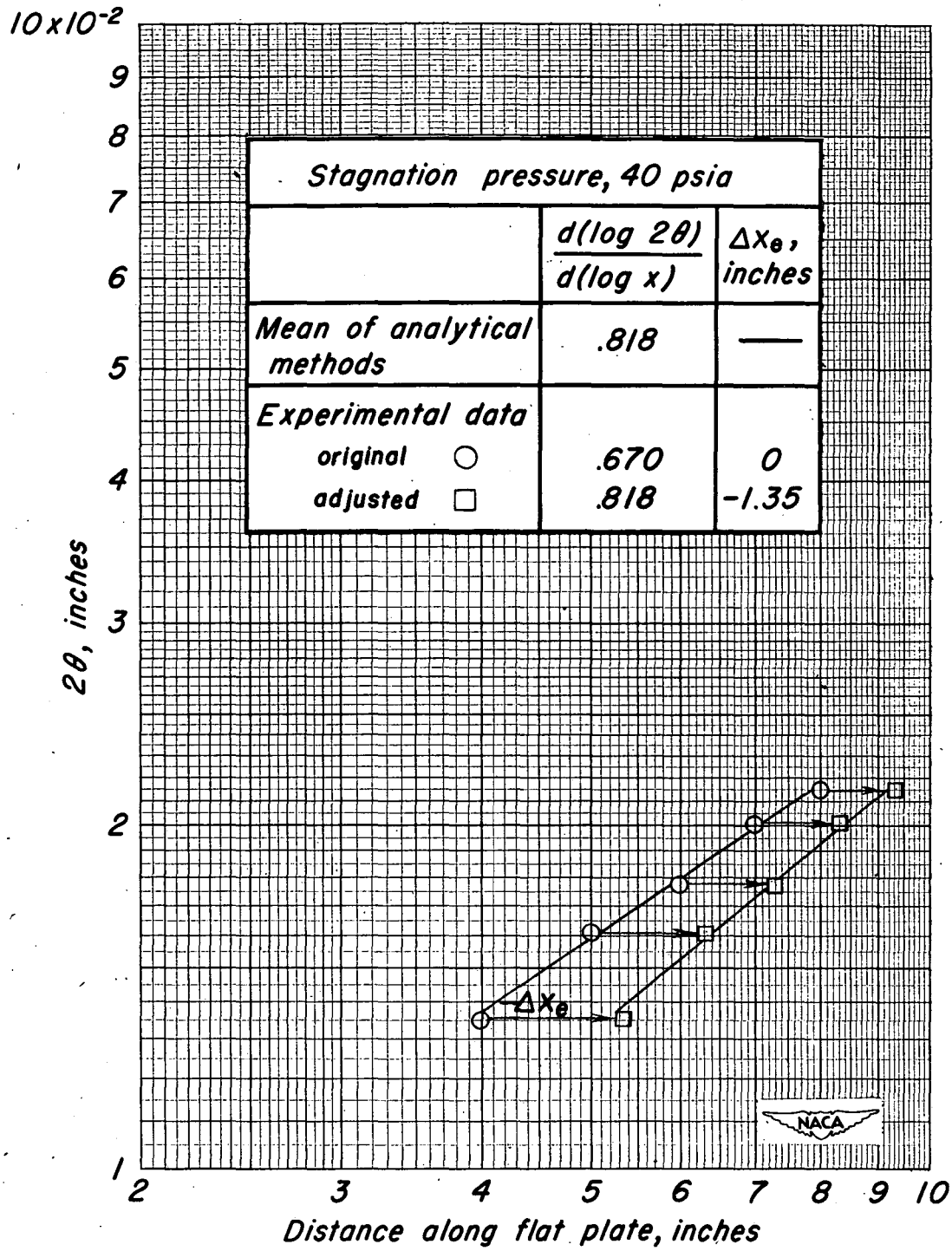


*Figure 6.– Method of determining effective starting length on flat plate model.*

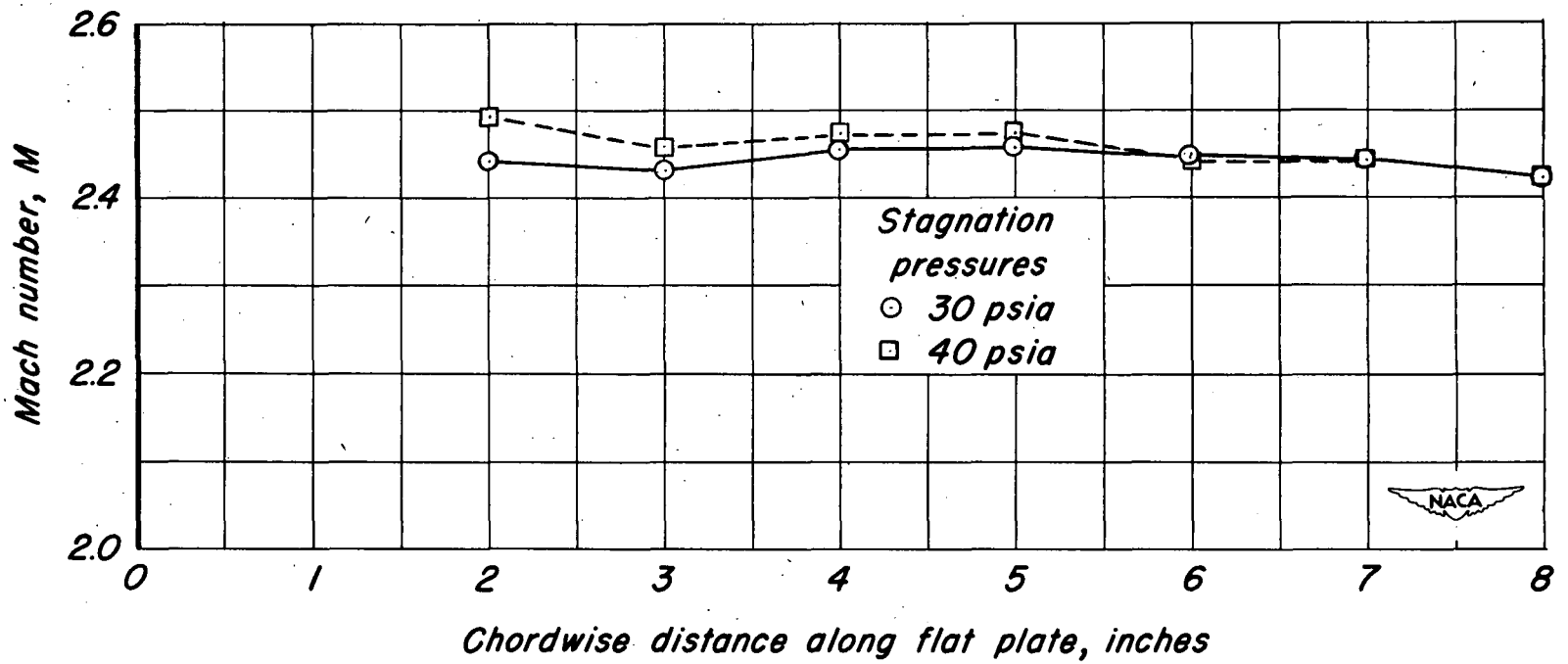


Figure 7.- Mach number distribution along the flat plate.

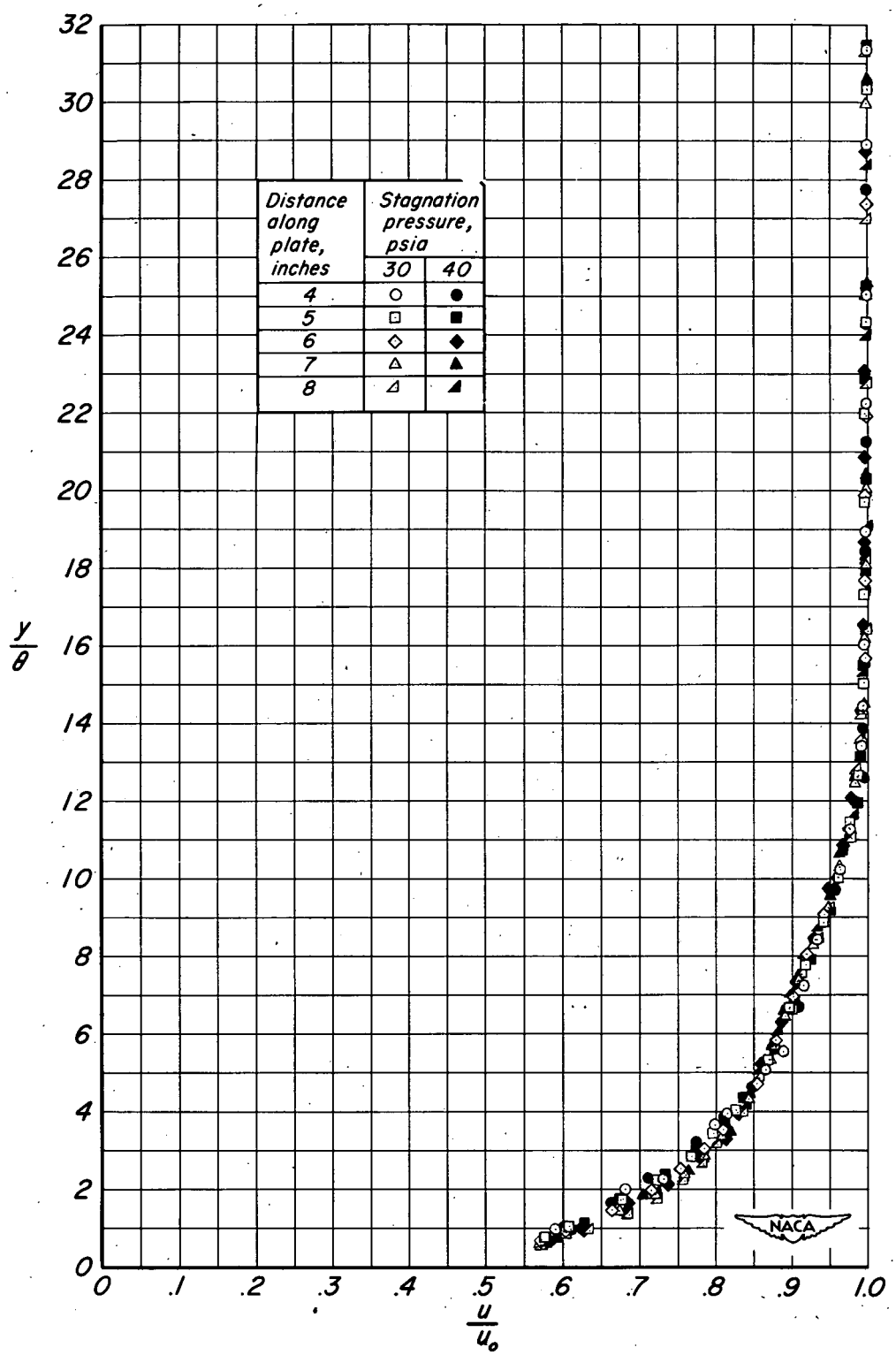


*Figure 8.– Velocity distributions in the boundary layer of the flat plate.*

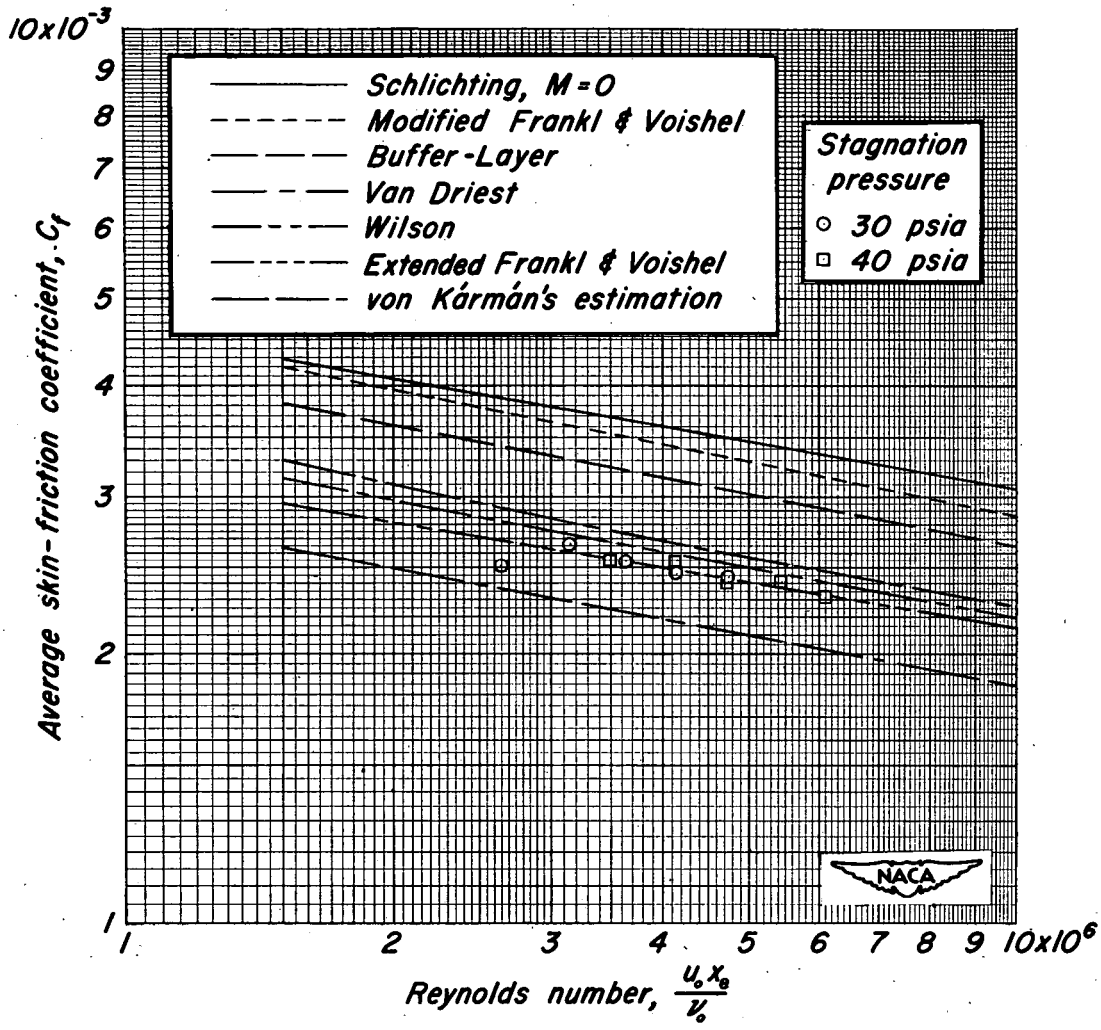


*Figure 9.– Comparison of several analytical methods with experimental skin-friction coefficients along a flat plate, M = 2.5.*

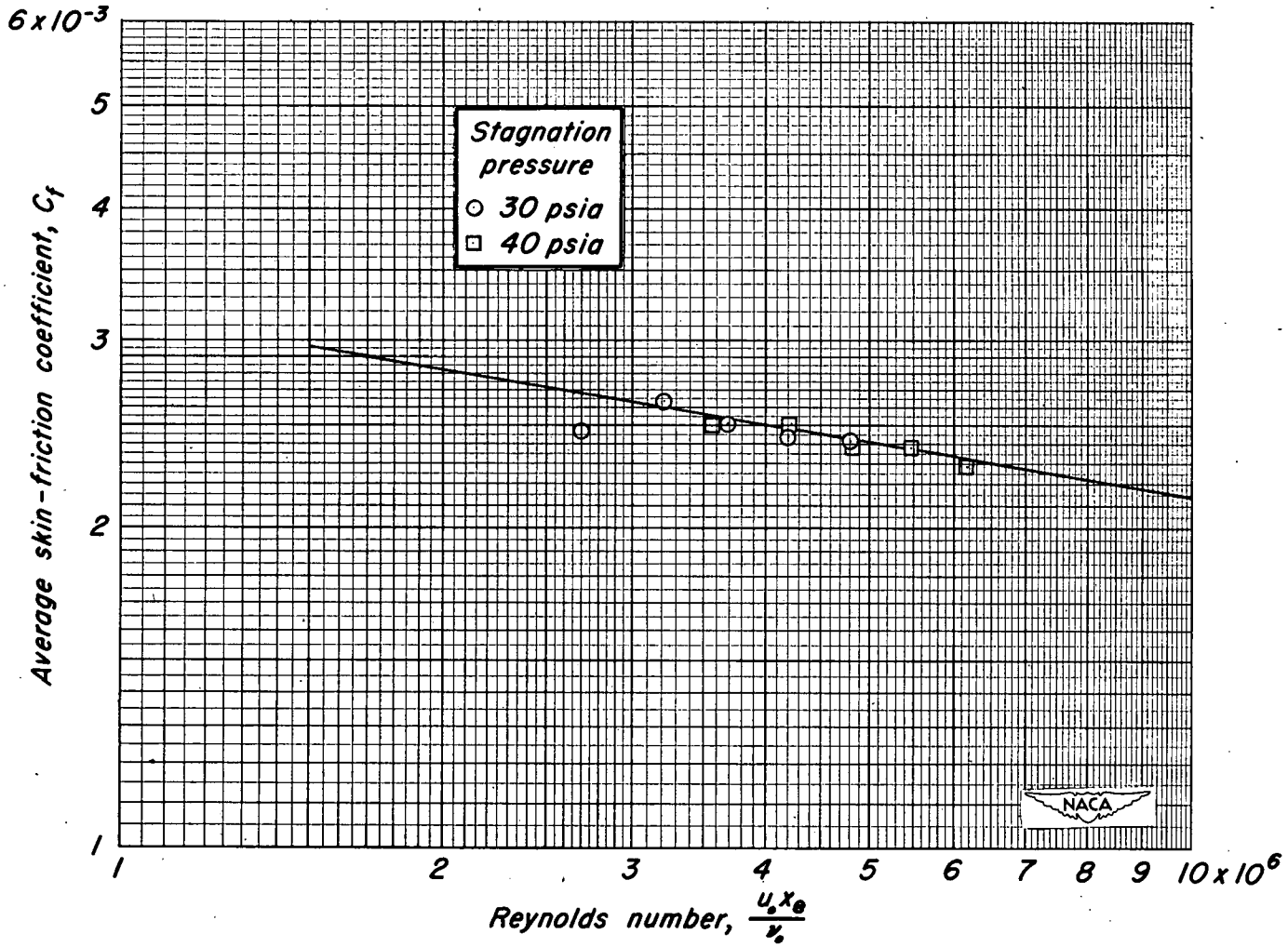


*Figure 10.- Final comparison of Frankl and Voishel, wall-properties, analytical method with experimental skin-friction coefficients along a flat plate, M = 2.5.*

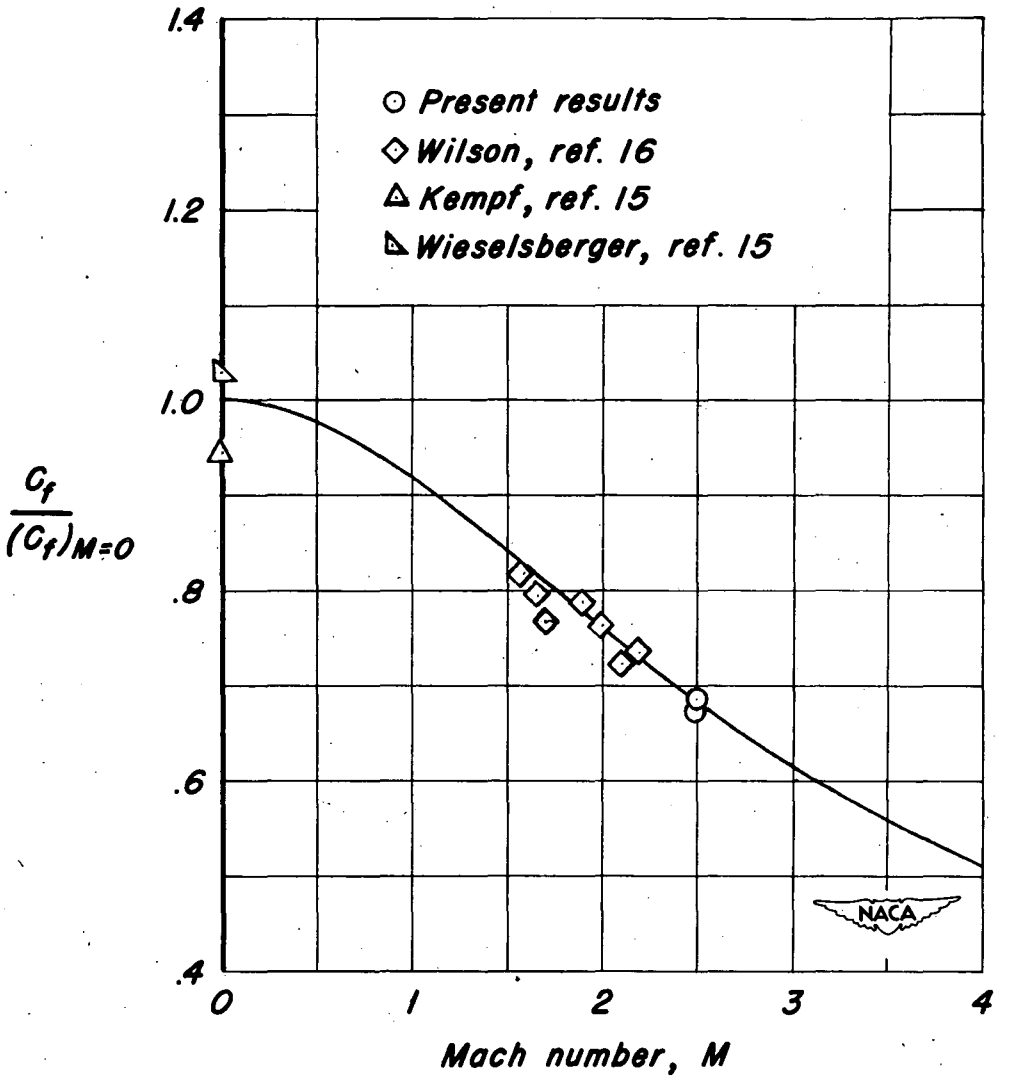


*Figure 11.- Comparison of Frankl and Voishel, wall-properties, analytical method with experimental average skin-friction coefficients along a flat plate with a turbulent boundary layer.*

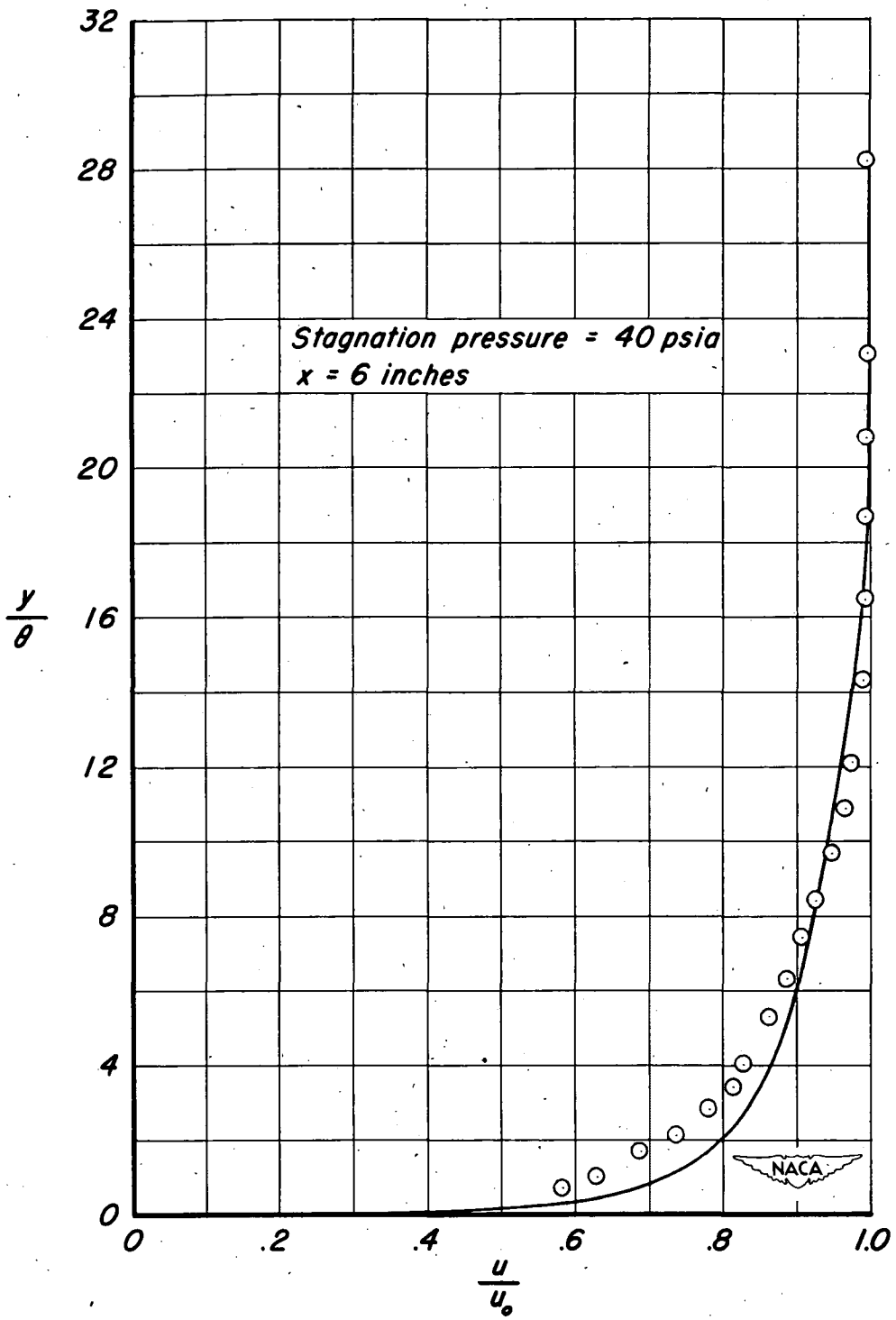


*Figure 12.- Comparison of Frankl and Voishel velocity distribution with an experimental velocity distribution in the boundary layer, M = 2.5 .*